JOURNAL OF CATALYSIS **106**, 23–37 (1987)

Acrolein Oxidation over 12-Molybdophosphates

III. Reaction Mechanism

E. M. SERWICKA, J. B. BLACK, AND J. B. GOODENOUGH

Inorganic Chemistry Laboratory, University of Oxford, South Parks Road, Oxford OX1 3QR, United Kingdom

Received April 17, 1986; revised January 27, 1987

ESR and IR measurements have identified the mechanism by which acrolein is oxidized to acrylic acid over $K_3PMo_{12}O_{40}$. Under dry conditions at room temperature, acrolein is physisorbed at a bridging oxygen of the Keggin $(PMo_{12}O_{40})^{3-}$ anion; the bridging oxygen makes a nucleophilic attack on the carbonyl carbon of the acrolein molecule. In air at room temperature, water adsorption competes for the active sites. In the temperature interval 293 K $< T <$ 453 K, the acrolein molecule becomes increasingly dissociatively chemisorbed to form an acrylate-type species, two electrons and a proton being transferred to the Keggin unit. Electron and proton transfer occurs between Keggin units, and the electron redistribution produces an ESR signal symmetric at 77 K that is typical for a Keggin unit reduced by one electron. Above 453 K, recapture of a proton by the acrylate anion produces acrylic acid desorption, which leaves the Keggin unit reduced and containing an oxygen vacancy at which a trapped electron gives an asymmetric Mo(V) signal. © 1987 Academic Press, Inc.

INTRODUCTION

In Part I of this series (*1*), it was established that catalysts $K_xH_{3-x}PMo_{12}O_{40} \cdot nH_2O$ in the compositional range $2.5 \leq x \leq 3.0$ consist, after calcination at 673 K, of well-formed particles having the cubic $K_3PMo_{12}O_{40}$ (K_3) structure and Keggin $(PMo_{12}O_{40})^{3-}$ polyanion units at the surface. The core of the particles is the K_3 phase; an epitaxial K_0 phase (i.e., $H_3PMo_{12}O_{40}$) at the surface introduces protons to the surface Keggin units, and the probability that these units carry one, two, or three protons increases with decreasing x.

In Part II (*2*), catalyst performance tests for all values of x were reported; these tests showed that the selectivity is enhanced by protonation of the intact surface Keggin units. This enhancement was rationalized on the basis of a Mars–van Krevelen selective oxidation mechanism according to which lattice oxygen is inserted into the organic molecule and gaseous oxygen subsequently reoxidizes the catalyst (*3*).

In the particular case of acrolein or methacrolein oxidation over heteropolymolybdates, Misono *et al.* (*4*) have provided compelling evidence for the Mars–van Krevelen mechanism; they have shown that selective oxidation products can be formed without oxygen in the feed stream, and they have used ^{18}O labeling to show that oxygen from the catalyst is incorporated into the acrylic acid product.

The Mars–van Krevelen mechanism requires that the metal oxide catalyst be able to accommodate at once both reduction of an active metal center and an associated decrease in its oxygen-coordination number. To follow the structural changes at a bulk-oxide surface is a difficult problem. However, where the active oxide surface is an intact Keggin unit of small size with a well-characterized structure, this problem becomes feasible. For such a study, catalyst compositions in the range $2.5 \leq x \leq 3.0$ are the most appropriate.

In this paper, a study of the reaction

0021-9517/87 $3.00

mechanism for the catalytic oxidation of acrolein to acrylic acid is reported. Direct identifications of both the organic-molecule reaction intermediates and the Keggin-unit changes at different stages of the reaction are presented. Such identifications at reactor temperatures are made difficult, if not impossible, by fast reaction kinetics. Therefore the investigation was carried out over a wide temperature range, from ambient up to a temperature, viz. 623 K, typical for a standard catalytic test. The several reaction steps were found to have threshold temperatures, which permitted separate characterizations of the physisorbed and chemisorbed organic species as well as of the Keggin unit (1) before reaction, (2) in relationship separately to the physisorbed and chemisorbed organic species, and (3) after desorption of the reaction product, but before reoxidation. The signatures of the gas-phase acrolein and of the two modes of acrolein adsorption were monitored by diffuse-reflectance IR and transmission IR spectroscopy; the structural and chemical properties of the surface Keggin unit at various stages of the reaction were followed by ESR spectroscopy and diffuse-reflectance IR spectroscopy.

EXPERIMENTAL

A. Catalysts

Samples of the K_x series were prepared as described in Part I (*1*), and the calcination was carried out at 673 K for 5 h.

B. Techniques

(*1*) *Electron-spin resonance.* ESR spectra were recorded at room temperature, 77 and 14 K, with a Varian E-112 Century-line spectrometer equipped with a fieldial and operating in the X band. DPPH was used as a standard for the determination of g factors. Spin concentrations were estimated by the double integration of the ESR signals with respect to a $VOSO_4$ standard.

(*2*) *Transmission infrared spectroscopy.* Spectra were recorded in the region 4000–400 cm^{-1} with a Perkin-Elmer 1710 Fourier transform IR spectrometer. Typically 5–10 scans were recorded with 2 cm^{-1} resolution. For adsorption experiments, the catalyst samples were placed in a glove bag filled with dry nitrogen. A few milliliters of acrolein were allowed to evaporate inside the bag for 10 min. The catalysts were then mulled with nujol and pressed into a thin film between KBr disks. IR spectra were run immediately after removal of the samples from the glove bag.

(*3*) *Diffuse-reflectance infrared spectroscopy.* Spectra were recorded on a Nicolet 2000 FT-IR spectrometer operating with a diffuse-reflectance cell attachment. This instrument was made available by I.C.I. plc (Wilton). Spectra were recorded at 4 cm^{-1} resolution, and typically 1000 scans were taken.

RESULTS

A. ESR Studies

(*1*) *Catalysts prior to exposure to acrolein.* According to ESR analysis, all calcined catalysts of the K_x series showed a small degree of reduction prior to exposure to acrolein. However, the character of the ESR signal changed with x.

The signal observed in calcined K_0 (i.e., $H_3PMo_{12}O_{40}$), illustrated in Fig. 1a, was discussed in Part I (*1*). It was assigned to a [Mo(V)=OO_4] cluster in MoO_3 (*5*) formed as a result of partial decomposition of the K_0 phase. This absorption was detectable at room temperature; recording at 77 K resulted in a better signal resolution. The amount of ESR-detectable Mo(V) corresponded to ca. 0.02% of the total amount of molybdenum present in the K_0 sample.

The signal observed in calcined K_0 was absent in the spectrum of the other end member of the K_x series, K_3, where the room-temperature recording did not reveal any paramagnetic species. At 77 K, however, a symmetric line of low intensity and $g = 1.957$ could be observed (Fig. 1b). It is argued below that this signal, denoted

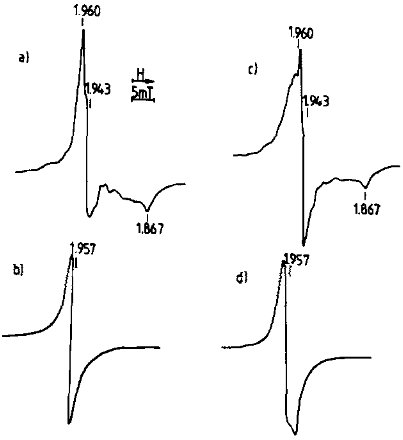

FIG. 1. ESR spectra of calcined catalysts: (a) K_0, (b) K_3, (c) K_2, and (d) $K_{2.75}$, recorded at 77 K.

hereinafter as signal S, corresponds to an unpaired electron delocalized over an entire Keggin unit. Its appearance can be associated with the presence of impurities (e.g., alkaline-earth cations substituting for K^+) that render the K_3 phase *n*-type. The amount of reduction was an order of magnitude lower than that observed for the K_0 sample, indicating an almost stoichiometric composition of the K_3 catalyst.

The ESR spectra of samples of intermediate compositions contained features characteristic of both signals discussed above, which is consistent with the two-phase analysis presented in Part I: they demonstrate the occurrence of K_3 and MoO_3 phases for all calcined samples with intermediate values of x. Figures 1c and 1d show, as examples, the ESR spectra of the calcined K_2 and $K_{2.75}$ catalysts.

(2) Catalysts after exposure to acrolein. Interaction of the calcined K_x series with acrolein vapor was studied in the temperature range 293–573 K under a pressure of 160 mm Hg (1 mm Hg = 133 Pa). The K_3 phase, being the only single-phase material, gave the least complex spectra.

Even room-temperature exposure of the calcined K_3 phase to acrolein vapor produced a change in the ESR spectrum at 77 K; the intensity of the weak signal S increased with exposure time, becoming an order of magnitude larger after room-temperature treatment for a period of several days. The signal was broadened beyond detection at room temperature. On the other hand, measurement at 14 K revealed signal asymmetry and traces of a hyperfine structure (Fig. 2, dashed line).

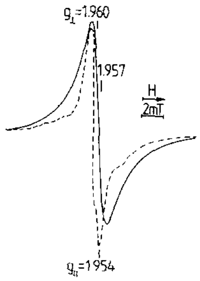

FIG. 2. ESR spectra of K_3 reduced with acrolein vapor for 24 h at room temperature, recorded at 77 K (continuous line) and 14 K (dashed line).

Both the temperature characteristics and the *g* values of this absorption are similar to those observed for frozen solutions of the 12-molybdophosphate anion (Fig. 3) reduced electrochemically by one electron (*6*). Such an electrochemical reduction introduces an electron to each Keggin unit without removal of an oxide ion. Consequently, the 12 molybdenum sites remain energetically equivalent so long as the single 4*d* electron per unit hops between molybdenum centers too rapidly to be

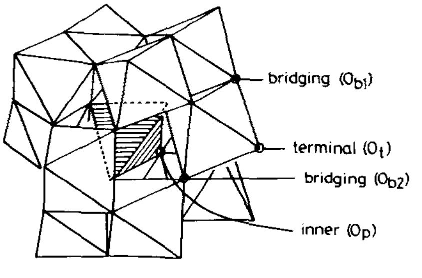

FIG. 3. Structure of the intact Keggin unit. Mo are displaced toward the terminal oxygen O_t; the two types of bridging oxygen, O_{b1} and O_{b2}, are referred to in the text as O_b.

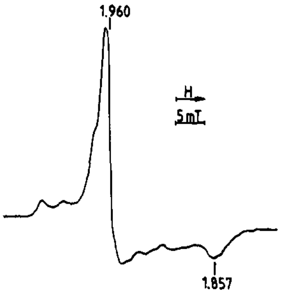

FIG. 4. ESR spectrum of K_3 reduced with acrolein vapor for 2 h at 453 K, recorded at room temperature.

trapped by a local atomic relaxation. As argued by Launay *et al.* (*6a*), the appearance of a symmetric line at 77 K, despite the obvious asymmetry of the local Mo(V) environment in the Keggin unit, indicates that, at this temperature, the electron hopping is fast relative to the time of an ESR measurement ($\tau_h < 10^{-8}$ s). Such a fast electron exchange between molybdenum sites having differently oriented magnetic axes is equivalent to a molecular tumbling; therefore, it gives an isotropic spectrum even in frozen solutions. Fast hopping at 77 K was confirmed by the observation of an asymmetric signal at 10 K with well-resolved $g_\perp$ and $g_\parallel$ and a hyperfine pattern that indicated localization of the unpaired electron on a single molybdenum nucleus at this temperature, at least on the time scale of an ESR experiment. Since the signal S of Fig. 2 shows exactly the same variation with temperature as well as similar ESR parameters, it is taken to represent the ESR signature of a Keggin unit reduced by a single electron without loss of an oxygen atom.

The observed growth of signal S upon adsorption of acrolein on the K_3 catalysts at room temperature indicates that the interaction is accompanied by a slow electron transfer to the solid, with no apparent loss of oxygen from the Keggin structure.

Exposure of the K_3 phase to acrolein vapor at higher temperatures, up to 423 K, caused increasingly rapid growth in the S signal intensity at 77 K, and the color of the sample was observed to change from yellow to green during exposure at 423 K.

After treatment at 453 K, a room-temperature asymmetric signal was detected (Fig. 4), even though signal S dominated the spectrum at 77 K. After exposure of the K_3 phase to acrolein at temperatures in the range $453 < T < 573$ K, the asymmetric signal became increasingly dominant at 77 K (Fig. 5). This asymmetric signal, hereinafter denoted signal A, is characterized by $g_1 = 1.960$, $g_2 = 1.969$ (both corresponding to $g_\perp$) and $g_3 = 1.857$ (corresponding to $g_\parallel$). The existence of hyperfine structure from isotopes ^{95}Mo (15.8% abundant) and ^{97}Mo (9.6% abundant), both of which have nuclear spin $I = \frac{5}{2}$, confirms that the signal is due to Mo(V). The hyperfine constants $A_1 = 4.35$ mT, $A_2 = 4.20$ mT, and $A_3 = 9.75$ mT were determined.

An almost identical ESR spectrum was obtained in a separate experiment for the K_3 sample reduced in vacuo at 673 K. The signal is similar to that reported by Otake *et al.* (*6b*) for K_0 reduced by H_2 at 553 K. Reduction under these conditions, accompanied by a color change from yellow to grayish-green, is obviously due to oxygen extraction from the catalyst. Therefore the asymmetric signal A is to be associated

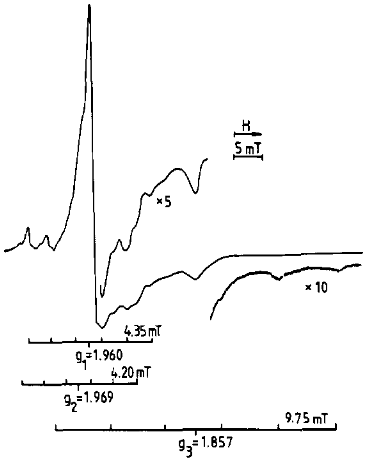

FIG. 5. ESR spectrum of K_3 reduced with acrolein vapor for 1 h at 573 K, recorded at 77 K.

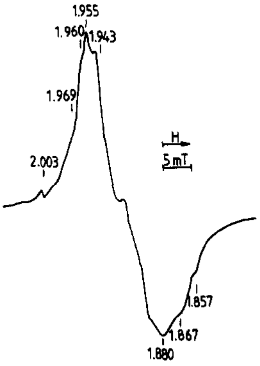

FIG. 6. ESR spectrum of K_1 reduced with acrolein vapor for 0.5 h at 473 K, recorded at 77 K.

with an oxygen-deficient Keggin unit. In the case of reduction with acrolein vapor, such a situation would arise at temperatures high enough for desorption of acrylic acid, a Keggin-unit oxygen being donated to the reaction product as envisaged in the Mars–van Krevelen mechanism. From our observations, it follows that a threshold temperature for such a desorption process to occur with a significant rate is around 453 K.

Signal A was also a predominant feature of calcined $K_{2.5}$ and K_2 samples that had been reduced with acrolein vapor at 473 K.

Reduction of the other members of the K_x series at 473 K led to more complicated spectra as x decreased. Figure 6 shows, as an example, the spectrum of a K_1 catalyst. Some of its features could originate from the reduced MoO_3 (5) and oxygen-deficient reduced Keggin units. However, other unidentified signals are also present, and all the features are considerably broadened. These results are consistent with the complex, multiphase character demonstrated in Part I (*1*) for the calcined catalysts with lower values of x.

(*3*) *Reducibility and reoxidation.* Reduction of calcined catalysts from the K_x series by exposure to acrolein vapor at 473 K for various periods of time followed by subsequent reoxidation revealed systematic variations in the reducibility and reoxidizability of the samples. In Fig. 7, the integral intensity of the ESR signal is used as a measure of the degree of reduction as a function of the time of exposure. The continuous lines represent, therefore, the kinetics of reduction, and the dashed lines the kinetics of reoxidation.

For all the catalysts studied, there is a rapid rise in the ESR-active Mo(V) concentration at the initial stages of reduction; the initial rise is followed by more gradual changes in the ESR signal intensity over the next few hours of treatment. The plots for K_0 and K_1 show that, for these samples, the integrated ESR signal decreases with increasing time after the initial reduction stage. A similar behavior has been reported (*7*) for MoO_3 reduced by propene. On reoxidation in air at 473 K, the ESR signal intensities from these two catalysts grow during the first hour before leveling off to a fairly constant value. Such behavior on reduction and/or reoxidation indicates that a considerable fraction of the electrons added on reduction are trapped at ESR-inactive two-electron sites that can be reoxidized reversibly to ESR-active one-electron sites. The ESR-inactive electrons could be trapped in Mo(V)–Mo(V) homopolar bonds or at a non-Kramers Mo(IV); they could also be spin-paired in a molecular orbital formed by larger

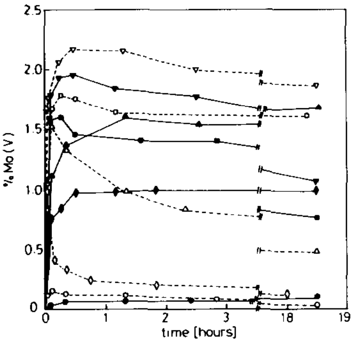

FIG. 7. Kinetics of reduction and reoxidation of K_x catalysts at 473 K as followed by ESR; continuous lines represent reduction, dashed lines reoxidation: (● ○) K_3; (◆ ◇) $K_{2.5}$; (▲ △) K_2; (■ □) K_1; (▼ ▽) K_0.

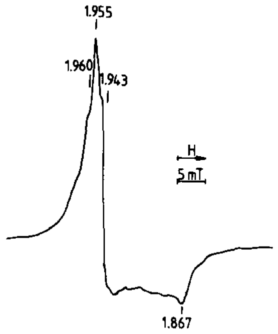

FIG. 8. ESR spectrum of K_1 after 18 h of reoxidation at 473 K, recorded at 77 K.

Mo-atom clusters. No Mo(III) was observed in the ESR spectra of these low-x samples.

The redox cycles of calcined K_2 and $K_{2.5}$ catalysts exhibit no decrease in ESR signal at the longer exposure times and no significant initial recovery of signal on reoxidation. The reducibility of the $K_{2.5}$ sample was smaller than that of the K_2 sample, and the $K_{2.5}$ sample was nearly completely reoxidized. Moreover, the majority of the ESR signal from the $K_{2.5}$ sample was signal A, which is characteristic of the oxygen-deficient Keggin unit.

The lineshapes of the ESR signals persisting after reoxidation suggest that the irreversible reduction is associated with decomposition products of the K_0 phase. Figure 8 shows the ESR signal present in the K_1 sample after 18 h of reoxidation. Features due to the [Mo(V)=OO_4] cluster in MoO_3 are clearly recognizable.

The level of reduction observed on treatment of a K_3 sample was much less than that observed for other samples; after prolonged exposure the signal observed was mainly asymmetric with a small component of symmetric signal S. Most of the asymmetric component of the signal could be removed on reoxidation.

B. IR Studies

(*1*) *Choice of catalyst.* Diffuse-reflectance IR spectroscopy was employed to investigate the model of acrolein adsorption at various temperatures and the site of attack on the Keggin unit. The catalyst chosen for these experiments was the neutral salt K_3. This catalyst is single phase with a well-defined structure. Moreover, it is a catalyst with the highest surface area of the K_x series (*1*), which makes it particularly suitable for adsorption studies. The K_3 samples used were of two types: one (CW) had been calcined in the standard way for 5 h at 673 K; the other (CD) was calcined in dry air for 5 h at 673 K. The BET surface area of both types was 30 m^2/g.

(*2*) *Room-temperature adsorption.* The transmission IR spectrum obtained after room-temperature adsorption of acrolein on a CW sample showed only a small band around 1700 cm^{-1} in addition to the bands due to the catalyst and nujol. Much clearer spectra of the adsorbed acrolein were obtained from the CD sample. Figure 9a shows the corresponding difference spectrum in the region 2000–1100 cm^{-1} which

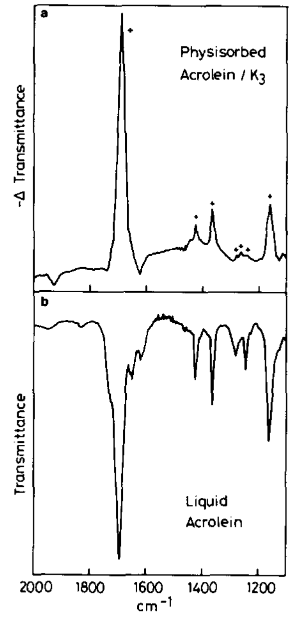

FIG. 9. (a) Transmission IR difference spectrum of acrolein adsorbed on K_3; bands positively identified are marked (+). (b) Transmission IR spectrum of liquid acrolein.

was obtained after subtracting the spectrum belonging to nujol and catalyst. For comparison, the spectrum of liquid acrolein in this spectral region, obtained from a thin film between KBr plates, is shown in Fig. 9b. The two spectra are seen to be essentially the same, which demonstrates that the extra bands observed after exposure to acrolein vapor are indeed due to adsorbed acrolein. The similarity of both spectra shows that this acrolein is physisorbed. Nevertheless, the physisorption was found to be strong enough to withstand 30 min of outgassing at room temperature. Observation of the weight change on adsorption of acrolein, followed in a separate experiment, gives a saturation acrolein coverage of 3–5 monolayers. On the other hand, the physisorbed acrolein was displaced rapidly on exposure to the atmosphere. Most of it was desorbed after 30 min exposure to air, and none could be detected after 45 min. In the same time interval, the intensities of the bands due to physisorbed water grew steadily, which indicates that it was the water present in the air that displaced the physisorbed acrolein.

(*3*) *Adsorption at 383 K.* The ESR studies indicated that electron transfer from acrolein to a Keggin unit occurs slowly at room temperature to enhance the symmetric signal S. Electron transfer would be associated with chemisorption, not physisorption, and the highest intensity of the ESR signal S was reached after prolonged exposure to acrolein at about 400 K. Therefore, similar conditions were applied to the calcined K_3 sample before taking the IR spectrum in order to optimize the possibility of detecting the chemisorbed species.

The transmission IR spectrum of Fig. 10 was recorded from a calcined sample of K_3 that had been exposed to acrolein at 383 K for several hours. This spectrum, obtained by interactive difference spectroscopy, shows a principal band from the adsorbed species (other than water) at around 1715 cm^{-1}; weaker bands are located at 1260, 1350, and 1400 cm^{-1}. None of these bands appear in the spectrum of physisorbed acrolein; they are therefore assigned to the chemically adsorbed form associated with electron transfer to the Keggin unit. The band at 1715 cm^{-1} indicates that the chemisorbed species retains a C=O double bond; the bands at 1400 and 1350 cm^{-1} can be associated with the CH_2 scissor vibration and the C–H in-plane bending vibration modes, respectively (*8*). The band at 1260 cm^{-1} may be assigned (see Discussion) as the asymmetric stretch of the O=C—O_b group in the chemisorbed species.

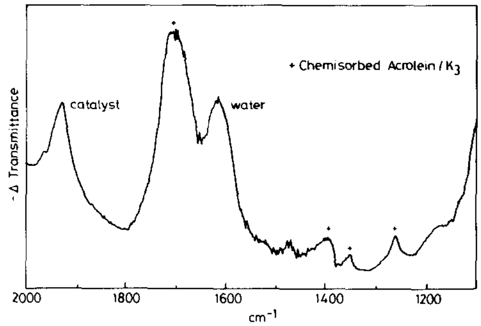

FIG. 10. Transmission IR difference spectrum of chemisorbed acrolein on K_3. Peaks positively assigned to the adsorbate are marked (+).

(*4*) *The Keggin unit.* Diffuse-reflectance IR spectroscopy was used to investigate changes occurring in the catalyst as a result of physisorption, chemisorption, and oxidized-product desorption, which leaves an oxygen vacancy in the Keggin unit.

A sample of calcined K_3 was placed in the diffuse-reflectance cell. After a brief evacuation, acrolein vapor was injected over the cell, which was then sealed and heated. The IR spectra recorded at 273, 473, and 623 K are presented in Fig. 11, which shows the region 1100–700 cm^{-1} where the bands most characteristic of the Keggin unit appear (*9*). These spectra clearly show that the Mo=O_t band (960 cm^{-1}) is essentially unchanged by this treatment whereas the bands due to Mo–O–Mo vibrations at 870 and 790 cm^{-1} are

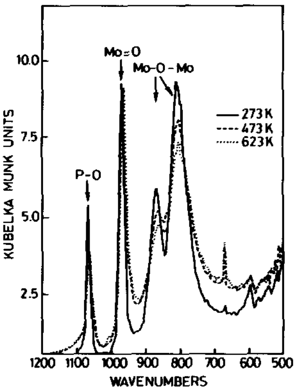

FIG. 11. Diffuse-reflectance IR spectra of K_3 reduced *in situ* with acrolein vapor at different temperatures. Wavenumber units are cm^{-1}.

broadened and reduced in intensity as the temperature is increased to where the Keggin unit is reduced, according to the ESR data, with the introduction of oxygen vacancies ($T \geq 453$ K). Similar changes in the IR spectrum of polymolybdophosphates reduced by methacrolein and hydrogen at high temperatures have been reported in the literature (*10*).

DISCUSSION

A. Interpretation of ESR Results

(*1*) *Acrolein-reduced K_3*. The ESR data demonstrate that acrolein reduces the polymolybdophosphate catalysts over the entire range of temperatures studied. The degree of reduction and the types of ESR spectra observed varied with temperature and the initial solid phases present.

Of particular interest for a microscopic description of the catalytic mechanism are the ESR data for the calcined K_3 sample after exposure to acrolein vapor at various temperatures. Exposure in the temperature interval $300 \leq T \leq 453$ K produced a strong increase of the symmetric signal S at $g = 1.957$, which is associated with a Keggin unit reduced by a single electron without loss of an oxygen atom. The rate of increase of signal S was slow at room temperature, but increased significantly with rising temperature. Since electron transfer implies chemisorption and the transition from physisorption to chemisorption would normally require a thermal activation, the data indicate that in this temperature range reduction of the Keggin unit of the K_3 phase without loss of oxygen is due to chemisorption. Although a chemisorbed species would reside at the surface of the Keggin unit, the appearance of signal S shows that the molybdenum atoms remain indistinguishable at 77 K in the reduced units. This is similar to the behavior found for those catalysts after low-temperature reduction by atomic hydrogen from a plasma discharge (*11*).

As shown below, acrolein chemisorption is dissociative with the transfer of two electrons and a proton to a Keggin unit from each adsorbed molecule. Since the electrochemical data show that signal S is to be associated with a Keggin unit reduced, without loss of oxygen, by only one electron, the observation of an increase in S with time of exposure to acrolein implies that electron migration, with or without an associated proton, is occurring between Keggin units. Direct evidence that such a migration is possible even at temperatures as low as 77 K comes from our experiments where K_x catalysts were reduced by atomic hydrogen (*11*); the results showed unambiguously that reduction proceeds into the bulk of the catalysts.

As the acrolein-exposure temperature is raised above 453 K, the asymmetric ESR signal A emerges increasingly with rising temperature and exposure time. Since signal A also occurs in the absence of acrolein after reduction of the K_3 catalyst at 673 K in vacuo, we may assign it to a Mo(V) atom trapped at an oxygen vacancy in the Keggin unit. In view of the observation by Misono *et al.* (*4*) that acrolein oxidation occurs via insertion of a lattice oxygen, the emergence of signal A on exposure to acrolein above 453 K can be associated with desorption of the oxidized product, acrylic acid.

Although desorption of acrylic acid leaves two electrons per oxygen vacancy in the catalyst, there was no direct evidence for two—or more—electrons at the oxygen-deficient Keggin unit. The possibility of two ESR-active Mo(V) ions trapped at the same oxygen vacancy is unlikely; such a configuration would give a broader linewidth than that observed for signal A. Therefore, where a Keggin unit carries an oxygen vacancy, we may conclude that two electrons in the same unit are ESR-inactive. Two explanations for this observation are plausible: either the formation of Mo(V)–Mo(V) dimers across the oxygen vacancy traps two spin-paired electrons in a molybdenum 4*d* molecular orbital or, alternatively, a disproportionation into Mo(IV) and Mo(VI) ions traps two ESR-silent electrons at a Mo(IV) ion. Electron–electron electrostatic interactions can be expected to favor the former model. No indication of Mo(III)-ion formation was found, and indeed Mo(III) in the presence of Mo(VI) is not expected.

The appearance of signal A after high-temperature reduction in acrolein vapor and/or vacuum thus indicates that the two electrons per oxygen vacancy left behind in the catalyst may be so distributed that, after desorption, Keggin units are left with only one ESR-active electron trapped as a Mo(V) at the oxygen vacancy. Moreover, strongly reduced samples give predominantly signal A, any contribution from signal S representing a much smaller fraction of intact Keggin units containing a single Mo-4*d* electron; therefore an electron transferred from an ESR-silent oxygen-deficient Keggin unit appears to go predominantly to singly occupied intact Keggin units, which become inactive if doubly occupied. The deduction that two electrons on an intact Keggin unit are spin-paired, and hence ESR-silent, is consistent not only with the observation of only signal S in the temperature range of chemisorption, but also with the report that solutions reduced electrochemically by two electrons per Keggin unit give unbroadened NMR spectra (^{17}O, ^{31}P) (*12*).

Finally, the ESR parameters for signal A, viz, $g_\perp > g_\parallel$ and $|A_\perp| < |A_\parallel|$, reveal the presence of a strong axial crystal-field component such as could only be established by formation of a multiple bond with a terminal oxygen. If the Mo=O$_t$ bonds are present at the Mo(V) adjacent to an oxygen vacancy, the missing oxygen must be a surface bridging oxygen O$_b$ (see Fig. 3). Removal of a bridging oxygen introduces a significant rhombic distortion of the Mo(V) site, which results in the observed splitting of $g_\perp$ into two separate values g_1 and g_2.

(2) *Crystal-field origins of signal A.* Fig. 12 illustrates the crystal-field energies for a Mo(V) ion in an intact Keggin unit. The cubic-field $^2T_{2g}$ and ^2E_g levels are primarily split by the displacement of the Mo from the center of symmetry toward a terminal oxygen O$_t$. This displacement introduces a strong tetragonal component to the crystalline field; the stronger σ and π bonding in the Mo=O$_t$ bond destabilizes the antibonding d_{z^2} and d_{yz}, d_{zx} orbitals relative to the $d_{x^2-y^2}$ and d_{xy} orbitals, where the z-axis is taken parallel to the Mo=O$_t$ bond axis. Reduction to Mo(V), which places a single electron in the d_{xy} orbital, does not perturb the formation of an oxomolybdenum group Mo=O$_t$; in fact, it tends to stabilize such a geometry for the Mo(V)-ion displacement, which is why the Mo(V) ESR spectra tend to exhibit a strong axial component to the g tensor. However, the electrostatic repulsion between the Mo atoms of a triangle of shared octahedral-site edges introduces a rhombic component, which lowers the point symmetry to C_{2v} or even C_s. At lower temperatures, ESR signal S becomes

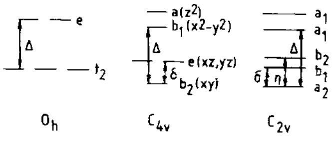

FIG. 12. Splitting of the Mo 4*d* orbitals in various symmetries.

asymmetric with a g tensor characteristic of the intact Keggin unit; the rhombic component of the crystalline field is too small to resolve the two components of $g_\perp$ in our experiments at 14 K.

On the other hand, removal of a bridging oxygen O_b in the xz plane enhances the rhombic component, so $g_\perp$ is resolved into g_1 and g_2 in signal A. Introduction of an oxygen vacancy on the x-axis also reduces the Mo–O bonding in the xy plane, thereby further stabilizing the a_2 orbital, which is mostly of d_{xy} character, and the lower a_1 orbital, which is mostly $d_{x^2-y^2}$ in character, relative to the other d levels. Stabilization of a_2 introduces an electron-trap site; stabilization of $d_{x^2-y^2}$ makes the lower a_1-orbital energy approach the b_2-orbital energy so as to obscure the relationship of the crystalline field of the distorted site to its octahedral origins.

(3) Reducibility and reoxidation. The data of Fig. 7 indicate that several of the multiphase components of the K_x system ($0 < x < 1$) interact with acrolein. For lower values of x, these phases include not only MoO_3 and phases initially containing stoichiometric Keggin units, but also intermediate phases that, on more extensive reduction, become reversibly ESR-inactive. For larger values of x, the Keggin units are increasingly more stable against degradation toward MoO_3 (*1*), and reoxidation is more complete. The stoichiometric Keggin unit is thus seen to be reduced by acrolein in a reversible manner. However, a reversible reduction of the K_3 sample that is only about 10% of that observed for the $K_{2.5}$ sample indicates that the Keggin unit is more reducible by acrolein when derived from a surface K_0 component, which supports the hypothesis (*1*, *2*) that a surface-stabilized K_0 phase is the active and selective component of an efficient catalyst.

B. Interpretation of IR Results

(1) Theoretical considerations. The ESR study identified two steps operative in the oxidation of acrolein over Keggin units, namely a chemisorption of acrolein that reduced the catalyst by charge transfer from the hydrocarbon molecule and a desorption of the product acrylic acid that left the catalyst both reduced and oxygen-deficient. Identification of the mode of acrolein adsorption and of the active catalyst sites was the aim of the IR studies. However, a theoretical orientation is useful at this stage of the discussion.

In the Keggin unit, the strong $Mo{=}O_t$ multiple bond, made evident by its short length, introduces sufficient π back-bonding from the anion to render the terminal oxygen O_t very acidic. The exposed bridging oxygens O_b are less acidic, and their lone pairs are more capable of performing a nucleophilic attack on a hydrocarbon molecule.

The HOMO at the Keggin-unit surface is a lone pair at the O_b atom. The LUMO of the unit is the Mo-4d orbital labeled a_2 in Fig. 12, but this orbital is relatively inaccessible to the acrolein as the surface oxygen atoms are close-packed.

The HOMO and LUMO of the acrolein molecule (*13*) are illustrated in Fig. 13; the overall charge distribution derived from the sum of the occupied-orbital coefficients (*14*) is also shown. The LUMO ($3a''$) is the first unoccupied orbital of the π-bond system; its largest coefficient is associated with the carbonyl carbon. The HOMO is the oxygen lone pair ($13a'$), but the $2a''$ orbital (essentially the $C{=}C$ π bond) lies very close to it in energy.

The initial interaction between acrolein and the Keggin unit, which is responsible for physisorption, would be dominated by an electrostatic attraction between the surface O_b and the carbonyl carbon. The reaction to form a chemisorbed species is governed by HOMO–LUMO interactions, of which there are two possibilities: (a) an electrophilic attack by the catalyst Mo-4d orbital a_2 on the acrolein $2a''$ (or possibly $13a'$) orbital and (b) a nucleophilic attack by the surface O_b on the $3a''$ orbital of

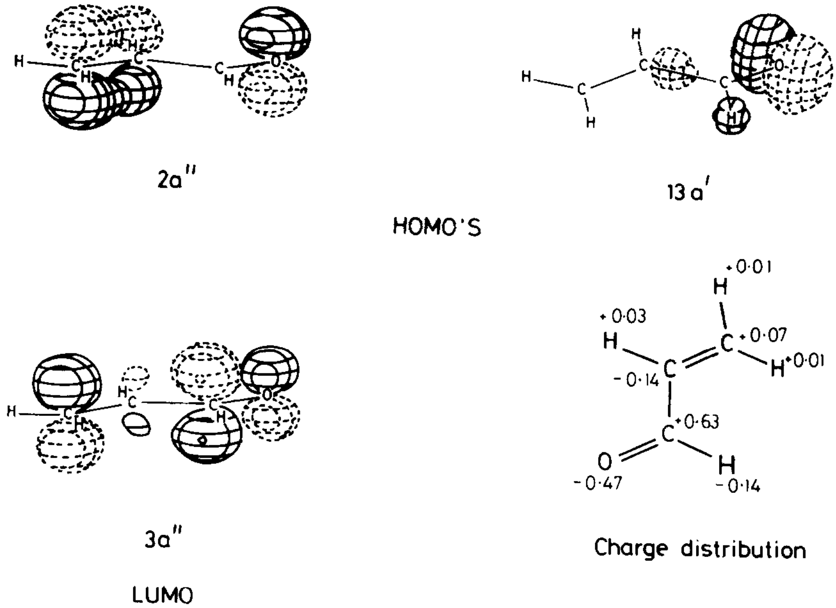

FIG. 13. Highest occupied and lowest unoccupied orbitals (from Ref. (13)), and charge distribution (from Ref. (14)) in the acrolein molecule.

acrolein. It is rare for aldehydes to react as nucleophiles, so the former pathway seems most unlikely in view of the added inaccessibility of the Mo-4*d* orbitals. On the other hand, a nucleophilic attack on the 3*a''* orbital is entirely possible.

(2) *Room-temperature adsorption.* As shown in Fig. 9, the IR spectrum of the acrolein molecule adsorbed at room temperature is similar to that of liquid acrolein, which confirms that the dominant adsorption mode at this temperature (in the absence of surface water) is physisorption. Although room-temperature evacuation demonstrated a relatively strong bonding of the physisorbed molecule, the rapid displacement of the molecule by water on exposure to air indicates that hydrogen bonding of the water molecules competes more strongly for the O_b sites. Therefore significant catalytic activity can only be anticipated at temperatures high enough [$T > 400$ K (1)] to remove adsorbed water from the surface of a Keggin anion. From the ESR studies, it is apparent that chemisorption occurs only slowly at room temperature.

(3) *Adsorption at 383 K.* As the temperature is raised from ambient to 400 K, the ESR data (signal S) indicate an increasingly rapid charge transfer to the Keggin unit without the introduction of an oxygen vacancy, which was interpreted to be firm evidence for chemisorption. The IR spectrum of Fig. 10 indeed reveals important structural aspects of the chemisorbed species: it retains a C=O stretch (band at 1715 cm^{-1}) and bands that can be assigned to a CH_2 scissor vibration and a C–H in-plane bending vibration. Nucleophilic attack by an O_b atom of the Keggin unit must therefore lead to a configuration of a chemisorbed species that preserves these features identified by the IR spectrum. Figure 14 depicts the likely reaction mechanism following nucleophilic attack at the carbonyl carbon of acrolein. Attack on the other electrophilic center (the β-carbon) can be discounted because (a) the coefficient of the LUMO is lower at this carbon

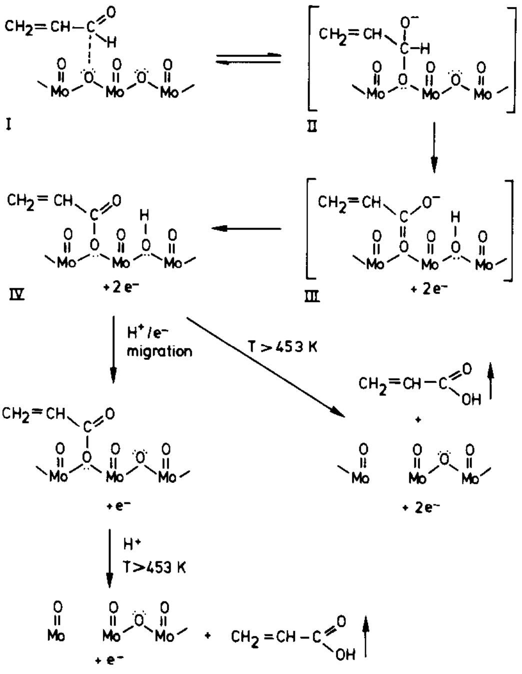

FIG. 14. Mechanism of acrolein interaction with a 12-molybdophosphate catalyst.

atom and (b) the proton abstraction required to make the oxidation reaction proceed would be far more difficult in this case.

Nucleophilic attack on the carbonyl carbon by the oxygen lone pair from the catalyst can be envisaged to proceed via the intermediate configurations II and III. Configuration II involves reaction of the LUMO of the acrolein molecule and the HOMO of the catalyst, but without charge transfer from the molecule to the Keggin unit. This intermediate would be short-lived, due to either the reverse reaction or the subsequent abstraction of aldehydic hydrogen, to give configuration III, which would involve the transfer of a proton and two electrons from the carbon–hydrogen bond to the catalyst via the carbon–oxygen π system. This step involves fission of the aldehyde C–H bond and therefore is not likely to be reversible. The carbonyl group would rapidly reform to give configuration IV, which is effectively an acrylate anion coordinated simultaneously to two molybdenum centers. This dissociative chemisorption transfers two electrons and a proton to the Keggin unit, and both the proton and the electrons are mobile species capable of migrating from one Keggin unit to another (*11*). The greater reducibility of a Keggin unit by acrolein in the presence of a surface proton suggests that the initial nucleophilic attack on the carbonyl carbon may be triggered by a proton transfer from the Keggin unit to the carbonyl oxygen.

Unassigned in the IR spectrum is a band at 1260 cm^{-1} that can be attributed to the asymmetric stretch of the $O–C–O_b$ unit. If the acrylate anion of configuration IV coordinating at O_b acts as a unidentate ligand, the IR stretching frequencies for the $O{=}C{—}O_bX$ unit would be intermediate between the extreme cases of the monomeric acrylic-acid molecule (X = H) and the free acrylate ion (X = lone pair). In the former case, formation of an O–H σ bond removes π character from the C–O bond to make the O=C—OH unit asymmetric. The vibrations that correspond to symmetric and asymmetric stretches of the acid group are, formally, the C–O single-bond and C=O double-bond stretches, respectively. In the latter case, both $C\overset{\cdots}{=}O$ bonds are equivalent and contain some π character.

Although systematic data on the IR spectra of unidentate acrylate ligands are not available, Robinson and Uttley (*15*) have summarized comparable data for a range of unidentate alkyl and aryl carboxylate ligands at platinum-metal centers. Changing the identity of R in RCOOX influences the stretching frequencies of the –COO– functional group because of inductive and conjugative effects, but these changes are much smaller (ca. 20–30 cm^{-1}) than those resulting from changes in the character of X. Therefore it is meaningful to make comparisons between compounds with different R. The range of values given in Ref. (*15*) are summarized in Table 1 together with values for free acrylic acid and the acrylate ion. It is clear that, as the equivalence of the two oxygen atoms is destroyed by the ligation of one oxygen to successively more pos-

TABLE 1

IR Frequencies (cm^{-1}) for the Acid Group in *R*COO*X* Compounds (Adapted from Ref. (*15*))

R	*X*	$\nu(OCO)_{sym}$	$\nu(OCO)_{asym}$
$CH_2{=}CH{-}$	H	1765, 1780	1240
Alkyl/aryl	Ru, Os, Rh, Ir	1580–1650	1310–1390
$CH_2{=}CH{-}$	Electron pair	1550	1440

itive species, the symmetric and asymmetric frequencies move apart and approach the C=O and C–O frequencies in free acrylic acid. The postulated structure, configuration IV of Fig. 14, of the chemisorbed species differs from the unidentate platinum-metal complexes only in that the coordinated oxygen O_b belongs to the coordination sphere of two, rather than one, metal centers; moreover, each of these metal centers carries a higher positive charge than that (typically +1) of the platinum metals studied in Ref. (*15*). Therefore the splitting between the two O—C—O_b stretch bonds should be much greater for the chemisorbed acrolein than was observed for the platinum-metal complexes.

The spectrum of Fig. 10 contains bands at 1715 and 1260 cm^{-1}. These two bands are closer than in the free monomeric acid (1765, 1780 cm^{-1} and 1240 cm^{-1}), but the splitting between them is greater than in the other carboxylate complexes. We can therefore associate these bands with the two O=C—O stretching frequencies of an adsorbed complex of the acrylic type.

(*4*) *The Keggin unit.* At temperatures $T \geq 473$ K, where desorption occurs to create oxygen vacancies in the Keggin structure, the IR spectra of the catalyst after exposure to acrolein show a decrease in intensity and a broadening of the Mo–O_b–Mo vibrations, but not of the Mo=O_t stretch, as is expected if the vacancies are at O_b sites and not O_t sites. However, the spectra show that the band at 1060 cm^{-1} due to the P–O_p stretch also falls in intensity even though the O_p atoms are deep in the Keggin unit. Pope (*16*) has reported that this band disappears on electrochemical reduction of the $[PW_{12}O_{40}]^{3-}$ anion; and Eguchi *et al.* (*10*) have shown that all the principal IR bands of the Keggin unit—except the Mo=O_t band—disappear gradually on reduction whether or not this reduction involves a loss of oxygen. They correctly argue that such an effect would occur simply as a result of the loss of tetrahedral symmetry, and such a symmetry loss is introduced by an O_b vacancy. It is also lost by the introduction of an electron having a $\tau_h > 10^{-12}$ s. Nevertheless these high-temperature IR data clearly show that the terminal oxygens O_t are not inserted into the product molecule; they are consistent with an O_b-atom insertion, which is the only other surface oxygen available.

C. Reaction Mechanism

From the foregoing discussions, including those in Parts I and II (*1, 2*), it is possible to argue definitively for the catalytic reaction mechanism summarized in Fig. 14.

The first step is physisorption of the acrolein molecule at an O_b atom via an interaction with the carbonyl carbon of the acrolein molecule. This adsorption mode is illustrated by configuration I; it must compete with water adsorption at temperatures $T < 400$ K.

Physisorption is followed by a dissociative chemisorption involving transfer of two electrons and a proton to the Keggin unit. This adsorption mode is illustrated as configuration IV. Chemisorption proceeds slowly at room temperature under dry conditions, but the proportion of chemisorbed to physisorbed species increases sharply with temperature so that at 383 K it was possible to obtain a well-resolved IR spectrum of the chemisorbed species (Fig. 10).

In the chemisorption mode, configuration IV, the transferred electrons hop rapidly with respect to the time of an ESR measurement ($\tau_h < 10^{-8}$ s), and electron–electron repulsions favor migration of an electron—with or without an associated proton—to a neighboring, intact Keggin unit. This migration creates Keggin units reduced by one electron which are ESR-active to give the ESR signal S.

At higher temperatures ($T \geq 453$ K), desorption of an acrylic acid molecule occurs on recapture of a proton by the "acrylate ion"; desorption leaves an oxygen vacancy at an O_b site and two electrons, at least one of which becomes trapped at a neighboring Mo to create an ESR-active Mo(V) responsible for the asymmetric signal A. Although we could not establish Mo(V)–Mo(V) dimerization if two electrons are trapped at the two Mo centers neighboring an O_b vacancy, nevertheless our data are not inconsistent with such a dimerization. The rate at which signal A is produced rises sharply with temperature for $T > 473$ K, where the thermal energy is large enough to induce desorption.

Reoxidation by a dioxygen molecule presumably creates a peroxide anion by reoccupation of the O_b vacancy and capturing one or two electrons. A peroxide anion contains a neutral oxygen that is mobile over the O_b sites and oxidatively active. If it encounters a chemisorbed species, it will react to give deep-oxidation products, thereby lowering the selectivity. Thus this active oxygen competes with mobile protons for capture by the chemisorbed species unless it is first intercepted by another active surface oxygen to form O_2, by protons to form H_2O, or by another oxygen vacancy. At higher conversion rates, the concentrations of mobile active oxygen and of chemisorbed species are both raised, so the probability of interception—other than by a desorbing product molecule—decreases and the selectivity falls.

Introduction of steam into the feed stream is known to enhance the selectivity (*17, 18*). If the oxygen of a water molecule enters an oxygen vacancy, it increases the proton concentration at the surface, thereby enhancing the selectivity.

The enhanced activity of the $K_{2.5}$ catalyst relative to the K_3 catalyst appears to be due to an epitaxial K_0 surface layer stabilized with respect to calcination. This layer would increase the surface proton density, imparting a Brønsted acidity that would be beneficial to the selectivity; it could also enhance physisorption if the surface layer is stabilized by proton transfer into the K_3 phase.

D. Final Comment

A particular feature of the reaction mechanism outlined in Fig. 14 is the use of metal atoms only as redox centers, not as adsorption sites. The fact that the reduced Mo(V) species is associated with a lower oxygen coordination is made possible by the stability of one or two short Mo–O bonds associated with a Mo(V) ion. This stability promotes acrylic acid desorption at a relatively low temperature.

This behavior is in marked contrast to the apparent role of the metal atoms in oxide catalysts for olefin oxidation. In olefin oxidation, adsorption is believed to occur via an electrophilic attack by a coordinatively unsaturated transition-metal center on the π system of the hydrocarbon species. A characteristic feature of the Keggin unit is the absence of any exposed transition-metal atom that can act as an adsorption site. Although coordinatively unsaturated Mo atoms appear after the initial reaction, the exposed metal atoms are displaced away from the vacancy. Nevertheless, electrophilic attack by these "exposed" Mo atoms may contribute to the loss of selectivity at higher conversions.

ACKNOWLEDGMENTS

We acknowledge the continuing interest in this program of Dr. John D. Scott, who made available the diffuse-reflectance IR facilities at I.C.I. PLC (Wilton), Mr. Neil Poole for assisting in these IR measurements, the Science and Engineering Research Council for a cooperative I.C.I.-Oxford University award, and the Institute of Catalysis, Polish Academy of Sciences, Kraków, for leave granted to Dr. Ewa M. Serwicka.

REFERENCES

1. Black, J. B., Clayden, N. J., Gai, P. L., Scott, J. D., Serwicka, E. M., and Goodenough, J. B., *J. Catal.* **106,** 1–15 (1987) [Part I].

2. Black, J. B., Scott, J. D. Serwicka, E. M., and Goodenough, J. B., *J. Catal.* **106,** 16–22 (1987) [Part II].
3. Mars, P., and van Krevelen, D. W., *Chem. Eng. Sci. Suppl.* **3,** 41 (1954).
4. Misono, M., Sakata, K., Yoneda, Y., and Lee, W. Y., "Proceedings, 7th International Congress on Catalysis, Tokyo, 1980," p. 1047. Kodansha (Tokyo)/Elsevier (Amsterdam), 1981.
5. Serwicka, E., *J. Solid State Chem.* **51,** 300 (1984).
6. (a) Launay, J. P., Fournier, M., Sanchez, C., Livage, J., and Pope, M. T., *Inorg. Nucl. Chem. Lett.* **16,** 257 (1980); (b) Otake, M., Komiyama, Y., and Otaki, T., *J. Phys. Chem.* **77,** 2896 (1973).
7. Dyrek, K., and Łabanowska, M., *J. Catal.* **81,** 46 (1983).
8. Bellamy, M. J., "The Infrared Spectra of Complex Molecules." Chapman and Hall, London, 1975.
9. Rocchiccioli-Deltcheff, C., Thouvenot, R., and Franck, R., *Spectrochim. Acta A* **32,** 587 (1976).
10. Eguchi, K., Toyozawa, Y., Yamazoe, N., and Seiyama, T., *J. Catal.* **83,** 32 (1983).
11. Serwicka, E. M., unpublished results.
12. Kazansky, L. P., Federov, M. A., Potapova, I. V., and Spitsyn, V. I., *Dokl. Akad. Nauk SSSR* **244,** 372 (1979).
13. Jorgensen, W. L., and Salem, L., "The Organic Chemist's Book of Orbitals," p. 181. Academic Press, New York/London, 1973.
14. Popova, G. Ya., Davydov, A. A., Zakharov, J. J., and Andrushkevich, T. V., *Kinet. Katal.* **23,** 692 (1982).
15. Robinson, S. D., and Uttley, M. F., *J. Chem. Soc., Dalton Trans.,* 1973, 1912.
16. Pope, M. T., "Proceedings, 5th International Conference on Chemistry and Uses of Molybdenum, Newcastle, 1985," unpublished.
17. Ai, M., *J. Catal.* **71,** 88 (1981).
18. Konishi, Y., Sakata, K., Misono, M., and Yoneda, Y., *J. Catal.* **77,** 169 (1982).